

## **$U(5) - SU(3)$ NUCLEAR SHAPE TRANSITION WITHIN THE INTERACTING BOSON MODEL APPLIED TO DYSPROSIUM ISOTOPES**

*M. Kotb*<sup>1</sup>

Physics Department, Faculty of Science, Al-Azhar University, Cairo

In the framework of the Interacting Boson Model (IBM) with intrinsic coherent state, the shape Hamiltonian from spherical vibrator  $U(5)$  to axially symmetric prolate deformed rotator  $SU(3)$  is examined. The Hamiltonian used is composed of a single-boson energy term and a quadrupole term. The potential energy surfaces (PES's) corresponding to the  $U(5)$ – $SU(3)$  transition are calculated with variation of scaling and control parameters. The model is applied to  $^{150-162}\text{Dy}$  chain of isotopes. In this chain, a change from spherical to well-deformed nuclei is observed when moving from the lighter to the heavier isotopes.  $^{156}\text{Dy}$  is a good candidate for the critical point symmetry  $X(5)$ . The parameters of the model are determined by using a computer simulated search program in order to minimize the deviation between our calculated and some selected experimental energy levels,  $B(E2)$  transition rates, and the two-neutron separation energies  $S_{2n}$ . We have also studied the energy ratios and the  $B(E2)$  values for the yrast state of the critical nucleus. The nucleon pair transfer intensities between ground–ground and ground–beta states are examined within the IBM and boson intrinsic coherent framework.

В работе исследуется изменение формы гамильтониана сферического вибратора  $U(5)$  при переходе к аксиально-симметричному вытянутому ротатору  $SU(3)$  в рамках модели взаимодействующих бозонов (МВБ) с внутренним когерентным состоянием. Используемый гамильтониан содержит член, описывающий энергию одного бозона, и квадрупольный член. Поверхности потенциальной энергии, соответствующие переходу  $U(5)$ – $SU(3)$ , вычисляются вариацией параметров скейлинга и контроля. Модель используется для описания изотопов цепочки  $^{150-162}\text{Dy}$ . В рассматриваемой цепочке наблюдается изменение от сферических к сильно деформированным ядрам при переходе от легких к более тяжелым изотопам. Изотоп  $^{156}\text{Dy}$  является хорошим кандидатом для наблюдения критической точки симметрии  $X(5)$ . Параметры модели вычисляются программой симулированного поиска минимума функции отклонения вычисленных значений уровня энергии, скорости перехода  $B(E2)$  и энергии отделения двух нейтронов  $S_{2n}$  от их экспериментальных значений. Также были исследованы отношения и значения  $B(E2)$  для yrast-состояния критического ядра. Вычислены интенсивности переходов нуклонных пар основа–основа и основа–бета-состояния в рамках МВБ и в предположении внутренней когерентности бозонов.

PACS: 21.60.Ev; 23.20.Lv; 27.70.+q

---

<sup>1</sup>E-mail: mahmoudkottb@gmail.com

## INTRODUCTION

The Interacting Boson Model (IBM) [1] provided us with an alternative description of nuclear collective excitations, which in contrast to the geometrical models, is of an algebraic nature. This realistic theoretical model was able to describe the low-energy collective states and the electromagnetic transitions of a large number of even–even nuclei successfully. In the original version of the IBM (IBM1), nuclei are regarded as systems composed of bosons, which carry either angular momentum  $L = 0$  ( $s$  bosons) or angular momentum  $L = 2$  ( $d$  bosons) [1]. The system of bosons, for which the number of bosons equals half the number of valence fermions  $N = n/2$  and interactions through a Hamiltonian that typically includes up to two-body interactions, is number conserving and rotationally invariant. The symmetry of the  $s$  and  $d$  bosons is the  $U(6)$  group structure; it has three solvable dynamical symmetries  $U(5)$ ,  $SU(3)$ , and  $O(6)$ , geometrically corresponding to spherical vibration, axial symmetric rotation, and  $\gamma$ -unstable rotation, respectively. These three dynamical symmetries are the vertices of the Casten triangle [2] that represents the nuclear phase diagram [3].

In the last few years, three transitional regions in atomic nuclei were studied [4–22], in particular, phase transition between the three dynamical limits of the IBM, transition from spherical  $U(5)$  to  $\gamma$ -unstable  $O(6)$ , and transition from well-deformed  $SU(3)$  to  $\gamma$ -unstable  $O(6)$ . The connection between the Bohr–Mottelson collective model [23] and the IBM comes from considering the IBM as the second quantization of the shape variables  $\beta$  and  $\gamma$  ( $\beta$  denotes the ellipsoidal deformation and  $\gamma$  is the measure of axial asymmetry). The intrinsic state formalism [24] was used. Phase transitions in nuclear shapes were observed at the boundary between regions characterized by different intrinsic shapes of quadrupole deformation.

Iachello [25–27] in his study of critical point behavior of nuclei introduced new dynamic symmetries called  $E(5)$  [25],  $X(5)$  [26], and  $Y(5)$  [27] critical point symmetries. The  $E(5)$  is designed to describe the critical point at the transition from spherical to deformed  $\gamma$ -unstable shapes. The potential to be used in the differential Bohr equation is assumed to be  $\gamma$ -independent, and for the  $\beta$  degree of freedom an infinite square well is taken. The  $X(5)$  and  $Y(5)$  are designed to describe the critical points between spherical and axially deformed shapes and between axial and triaxial deformed shapes, respectively. Bonatsos et al. [28] introduced the  $Z(5)$  critical point symmetry for the prolate-to-oblate nuclear shape transition.

To understand the shape phase transition in isotopic chains of nuclei, authors usually used the most general IBM Hamiltonian up to two-body terms using the creation-annihilation or the multipole forms. These forms contain many parameters (at least seven). In the present work, an alternative approach is used, a very simple Hamiltonian contains two terms and two parameters restricted to only one control parameter adapted to study the behavior of critical points in the  $U(5)$ – $SU(3)$  transition. The corresponding PES will be given by the expectation value of this Hamiltonian in the intrinsic coherent state. The predictions of the  $X(5)$  critical point symmetry for different observables are consistent with the results of the IBM Hamiltonian procedure. The paper is concentrated on the  $U(5)$ – $SU(3)$  shape transition by using the IBM with intrinsic coherent states. The paper is organized as follows. In Sec. 1, the IBM Hamiltonian, the intrinsic coherent state, and PES's identifying the shape transition are described. The location of the critical points in the shape transition is identified in Sec. 2. In Sec. 3, the proposed model is applied to Dy isotopic chain and the numerical results are discussed. Finally, a conclusion is given.

### 1. INTERACTING BOSON MODEL DESCRIPTION AND POTENTIAL ENERGY SURFACES (PES's) FOR THE $U(5)-SU(3)$ SHAPE TRANSITION

We start with the simplified transitional Hamiltonian that includes spherical and deformed terms of the form

$$H = \epsilon_d \hat{n}_d + k \hat{Q} \cdot \hat{Q}, \quad (1)$$

with the usual  $d$ -boson number operator  $\hat{n}_d$  and the usual  $SU(3)$  generator quadrupole operator  $\hat{Q}$  defined by

$$\hat{n}_d = \sum_{\mu} d_{\mu}^{\dagger} \tilde{d}_{\mu}, \quad (2)$$

$$\hat{Q} = [s^{\dagger} \times \tilde{d} + d^{\dagger} \times \tilde{s}]^{(2)} + \chi [d^{\dagger} \times \tilde{d}]^{(2)}. \quad (3)$$

For introducing geometry into the IBM, the following boson creation operator for axial symmetry nuclei is usually used:

$$\Gamma_c^{\dagger}(\beta) = \frac{1}{\sqrt{1+\beta^2}} [s^{\dagger} + \beta d_0^{\dagger}], \quad (4)$$

where  $\Gamma^{\dagger}$  is the boson creation operator acting in the intrinsic system and  $\beta$  is the quadrupole deformation parameter describing the geometrical shape.

We regard the normalized state [29]

$$|c\rangle = \frac{1}{\sqrt{N!}} (\Gamma^{\dagger}(\beta))^N |0\rangle \quad (5)$$

as an intrinsic coherent normalized state for the  $sd$  IBM for a nucleus with  $N$  valence bosons outside a doubly closed shell state  $|0\rangle$  (the boson vacuum).

We use  $|c\rangle$  as a variational trial function in constructing the potential energy surface (PES)

$$E(N, \beta) = \langle c | H | c \rangle = \epsilon_d \frac{N\beta^2}{1+\beta^2} + k \left\{ \frac{N}{1+\beta^2} [5 + (1+\chi^2)\beta^2] + \frac{N(N-1)}{(1+\beta^2)^2} \left[ 4\beta^2 - 4\sqrt{\frac{2}{7}}\chi\beta^3 \cos 3\gamma + \frac{2}{7}\chi^2\beta^4 \right] \right\}. \quad (6)$$

It has the following general form [4, 5] for  $\gamma = 0$ :

$$E(N, \beta) = N \frac{A_2\beta^2 + A_3\beta^3 + A_4\beta^4}{(1+\beta^2)^2} + A_0, \quad (7)$$

where the coefficients  $A_2$ ,  $A_3$ ,  $A_4$ , and  $A_0$  have the following linear combinations of the Hamiltonian parameters  $\epsilon_d$  and  $k$ :

$$A_2 = \epsilon + (4N + \chi^2 - 8)k, \quad (8)$$

$$A_3 = -4\sqrt{\frac{2}{7}}\chi k(N-1), \quad (9)$$

$$A_4 = \epsilon + \left( \frac{2N+5}{7}\chi^2 - 4 \right) k, \quad (10)$$

$$A_0 = 5k. \quad (11)$$

Introducing the control parameter  $y$  defined as

$$\frac{k}{\epsilon} = -\frac{y}{1-y}, \quad (12)$$

we arrive at the standard two-dimensional parameterization of the  $Q$ -consistent IBM Hamiltonian (1) which depends on only one control parameter  $y$ :

$$H = (\epsilon - k)[(1 - y)\hat{n}_d - yQ \cdot Q]. \quad (13)$$

For  $y = 0$ , we get the  $U(5)$  limit and for intermediate values of the control parameter  $y$ , the energy surface function will describe a certain point on the IBM symmetry triangle. In general, there is a spherical-deformed first-order phase transition as a function of  $y$ . The PES takes the general form

$$E(N, \beta) = \lambda \frac{a\beta^2 + b\beta^3 + c\beta^4}{(1 + \beta^2)^2} + d, \quad (14)$$

where

$$a = (1 - y) - (4N + \chi^2 - 8)y, \quad (15)$$

$$b = 4\sqrt{\frac{2}{7}}\chi y(N - 1), \quad (16)$$

$$c = (1 - y) - \left(\frac{2N + 5}{7}\chi^2 - 4\right)y, \quad (17)$$

$$d = -5y, \quad (18)$$

$$\lambda = (\epsilon - k)N. \quad (19)$$

## 2. CRITICALITY CONDITIONS

Minimizing of the PES equation (14) with respect to  $\beta$  for the given values of the control parameter  $y$  gives the equilibrium value  $\beta_0$  defining the phase of transition ( $b^2 = 4ac$ ).

The condition to find the antispinodal point is  $\left(\frac{d^2 E}{d\beta^2}\right)_{\beta=0} = 0$  and gives the relation  $a = 0$ . Thus,

$$y_{\text{ant}} = \frac{1}{4N - \chi^2 - 7}. \quad (20)$$

For  $\chi = -\sqrt{7}/2$ ,  $y = 1/((4N - 21)/4)$ .

If we eliminate the contribution of the one-body terms of the quadrupole–quadrupole interaction  $N \left(5 + \frac{11}{4}\beta^2\right) / (1 + \beta^2)$ , the coefficients in the PES for large- $N$  limit of the IBM read as

$$a = (1 - y) - 4Ny, \quad b = 4\sqrt{\frac{2}{7}}\chi Ny, \quad c = (1 - y) - \frac{2}{7}\chi^2 Ny.$$

The critical point (when  $b^2 = 4ac$ ) is located at  $y_c$  extracted from the equation

$$\left[ \left( 4 + \frac{2}{7}\chi^2 \right) N + 1 \right] y^2 - \left[ \left( 4 + \frac{2}{7}\chi^2 \right) N + 2 \right] y + 1 = 0. \tag{21}$$

At  $y_c$  the depth of the  $\beta = 0$  and  $\beta \neq 0$  minima becomes equal. The antispinodal point, where  $\beta \neq 0$  the minimum disappearance occurs, when  $a = 0 \left( \left( \frac{\partial^2 E}{\partial \beta^2} \right)_{\beta=0} = 0 \right)$ , that is at

$$y_a = \frac{1}{4N + 1}.$$

This antispinodal point follows shortly before the critical point  $y_a < y_c$ .

Taking the first-order derivative of the PES with respect to  $\beta$  and equating it to zero, we get the shape equilibrium equation for  $\chi = -\sqrt{7}/2$ :

$$2a + 3b\beta + (4c - 2a)\beta^2 - b\beta^3 = 0,$$

which leads to

$$[(1 - y) - 4Ny] - 3\sqrt{2}Ny\beta + [(1 - y) + 3Ny]\beta^2 + \sqrt{2}Ny\beta^3 = 0. \tag{22}$$

For the  $U(5)$  limit, with  $y = 0$ , the equilibrium deformation parameter  $\beta_0 = \pm i$ , that is no real  $\beta$  exists for the  $U(5)$  limit. This means that the  $U(5)$  limit corresponds to a spherical vibrator shape.

For the  $SU(3)$  limit, with  $y = 1$ , the cubic equation becomes

$$4 + 3\sqrt{2}\beta - 3\beta^2 - \sqrt{2}\beta^3 = 0$$

and the allowed parameter is  $\beta = \sqrt{2}$ .

The variation of the order parameter  $\beta$  with respect to the control parameter  $y$  in Eq. (22) is illustrated in Fig. 1. The characteristic cycle of the order parameter when the first-order phase transition takes place is observed. Spherical hysteresis phase ( $\beta = 0$ ) is up to  $y = 0.2$  and then the system jumps to the deformed minimum.

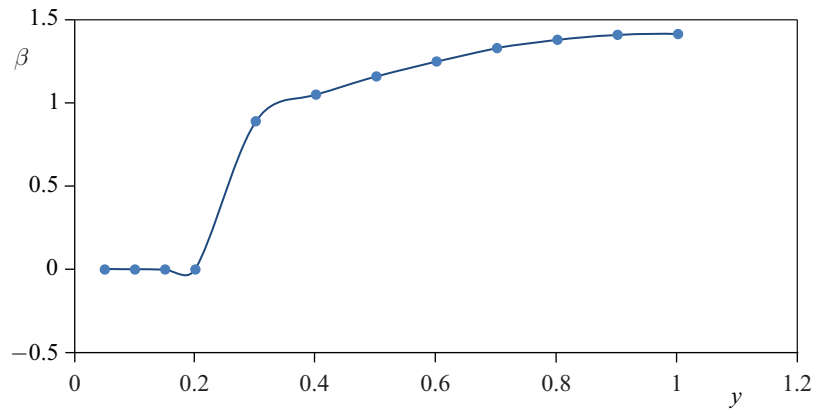


Fig. 1. Shape phase diagram for the  $U(5)$ – $SU(3)$  transition. The behavior of deformation parameter  $\beta$  with control parameter  $y$

For large- $N$  limit, the parameters  $a$ ,  $b$ , and  $c$  become

$$a = \left[ \frac{1-y}{Ny} - 4 \right] Ny, \quad b = -2\sqrt{2}Ny, \quad c = \left[ \frac{1-y}{Ny} - \frac{1}{2} \right] Ny.$$

Solving Eq. (21),  $b^2 = 4ac$  for  $\chi = -\sqrt{7}/2$ , yields the solutions  $y = 1$ ,  $y = 2/(9N + 2)$ , and the equilibrium values  $\beta_0 = 0$  and  $\beta_0 = 1/(2\sqrt{2})$ .

The PES takes the form

$$E_{\text{crit}} = \text{const} \frac{\beta_0^2 \left( \beta_0 - \frac{1}{2\sqrt{2}} \right)^2}{(1 + \beta^2)^2}. \quad (23)$$

The PES involves spherical minimum at  $\beta = 0$  and a prolate deformed minimum at  $\beta_0 = 1/(2\sqrt{2})$ .

Figure 2, *a* shows the behavior of the scaled PES  $E(\beta)$  near the minimum at  $\beta = 0$  and  $\beta_0 = 1/(2\sqrt{2})$  for  $((1-y)/(Ny))_c = 9/2$ , it approaches a constant for large  $\beta$ . The position and height of the barrier separating the two minima are given by

$$\beta = \frac{-1 + \sqrt{1 + \beta_0^2}}{\beta_0} = 3 - 2\sqrt{2}, \quad (24)$$

$$h = \left( \frac{-1 + \sqrt{1 + \beta_0^2}}{\beta_0} \right)^2 = \frac{1}{32}(17 - 12\sqrt{2}). \quad (25)$$

The symmetric phase takes place at  $y = 0$ , because the PES has a unique minimum at  $\beta = 0$ . When  $y$  increases, one reaches the spinodal point at  $(1-y)/(Ny) = 5$  (Fig. 2, *b*), where the second local nonsymmetric minimum at  $\beta \neq 0$  arises, it pushes the symmetric one till both attain the same depth at the critical point  $y = 2/(9N + 2)$  (Fig. 2, *a*). Beyond this value, the symmetric minimum at  $\beta = 0$  becomes the local minimum till  $(1-y)/(Ny) = 4$  (Fig. 2, *c*), where it becomes unstable antispinodal point.

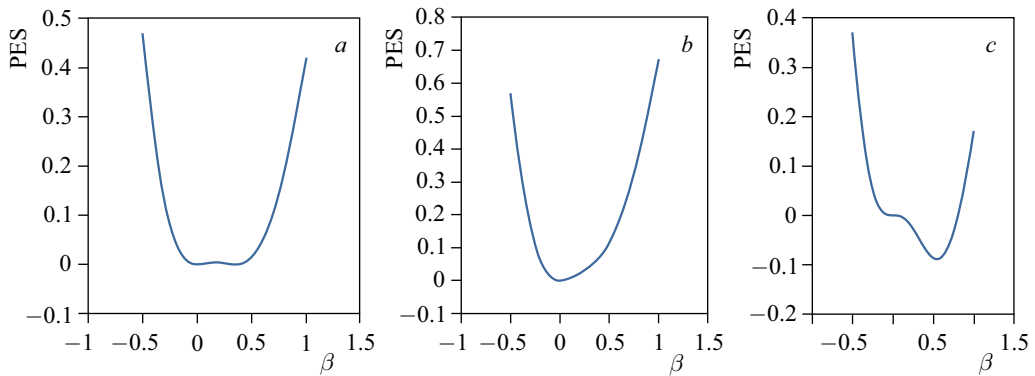


Fig. 2. A plot of the scaled PES in the large- $N$  limit and  $\chi = -\sqrt{7}/2$  as a function of deformation parameter  $\beta$  (phase diagram). The critical point  $((1-y)/(Ny))_c = 4.5$  is represented in plot *a*. Plots *b* and *c* show the two cases  $(1-y)/(Ny) = 5$  and  $(1-y)/(Ny) = 4$

### 3. NUMERICAL CALCULATIONS APPLIED TO EVEN-EVEN Dy ISOTOPES

In order to determine the best model parameters  $y$ ,  $\chi$ , and  $\lambda$  for each nucleus of Dy isotopic chain  $^{150-162}\text{Dy}$ , some experimental values of energy levels and  $B(E2)$  transition probabilities are selected and fitted with the IBM calculated ones by minimizing the mean square deviation using a computer simulated search program. The entire procedure is repeated for a new set of parameters, until a reasonable compromise is found between the theoretical and experimental ones. The mean square deviation in the energy and  $B(E2)$  values are quantified with the common definition of the chi squared

$$\chi_E^2 = \frac{1}{N_E} \sum_i \frac{(E_i^{\text{exp}} - E_i^{\text{cal}})^2}{(\text{exp. errors})^2}, \quad (26)$$

$$\chi_{B(E2)}^2 = \frac{1}{N_{B(E2)}} \sum_i \frac{(B(E2)^{\text{exp}} - B(E2)^{\text{cal}})^2}{(\text{exp. errors})^2}, \quad (27)$$

where  $N$  is the number of experimental points entering into the fitting procedure. Only six lowest levels  $I_i^\pi = 0^+, 2^+, 4^+, 6^+, 8^+, 10^+$  are used, because the model cannot be applied over an energy range including the band crossing. The experimental data are taken from the national nuclear data center [30]. Table 1 lists the adopted best set of parameters in the Hamiltonian for  $^{150-162}\text{Dy}$  isotopic chain. The PES's calculated by using the Hamiltonian equation (14) to describe the  $U(5)-SU(3)$  transition for isotopic chain  $^{150-162}\text{Dy}$  are illustrated in Fig. 3. The potentials are shown as a function of deformation parameter  $\beta$  along the axial trajectory  $\gamma = 0, 60^\circ$ . The corresponding model parameters are listed in Table 1. Here, we observe the shape transition from spherical nucleus  $^{150}\text{Dy}$  to well-deformed prolate nuclei  $^{158-162}\text{Dy}$ . We remark that the PES is not flat, exhibiting a deeper minimum in the prolate ( $\beta > 0$ ) region and a shallower minimum in the oblate ( $\beta < 0$ ) region. Relatively flat PES occurs for  $^{156}\text{Dy}$  nucleus (boson number  $N = 12$ ), suggested as a good example of the  $X(5)$  critical point symmetry. The isotopic chain passes from  $U(5)$  to  $SU(3)$  limit when the number of bosons is increasing from  $N = 9$  to  $N = 15$ .

**Table 1. The adopted best model parameters  $y$ ,  $\chi$ , and  $\lambda$  as derived in fitting procedure used in the calculations for the Dy isotopic chain for the  $U(5)-SU(3)$  shape transition**

Parameter	$^{150}\text{Dy}$	$^{152}\text{Dy}$	$^{154}\text{Dy}$	$^{156}\text{Dy}$	$^{158}\text{Dy}$	$^{160}\text{Dy}$	$^{162}\text{Dy}$
$N$	9	10	11	12	13	14	15
$y$	0.0333	0.041	0.0536	0.06	0.0576	0.06	0.0653
$\chi$	-1.32	-1.32	-1.1	-0.86	-0.8	-0.53	-0.3
$\lambda$	14.51	16.212	17.336	16.21	19.17	20.178	21.405

One of the best signatures of a shape transition is the behavior of the yrast excitation energy ratios  $R_{I+2/2} = E(I+2)/E(2_1^+)$  along the isotopic chain. The ratios for  $U(5)$  and  $SU(3)$  dynamical symmetry limits are given by

$$R_{I+2/2} = \begin{cases} \frac{I+2}{2} & \text{for } U(5), \\ \frac{(I+2)(I+3)}{6} & \text{for } SU(3), \end{cases} \quad (28)$$

with  $I = 0, 2, 4, 6, \dots$

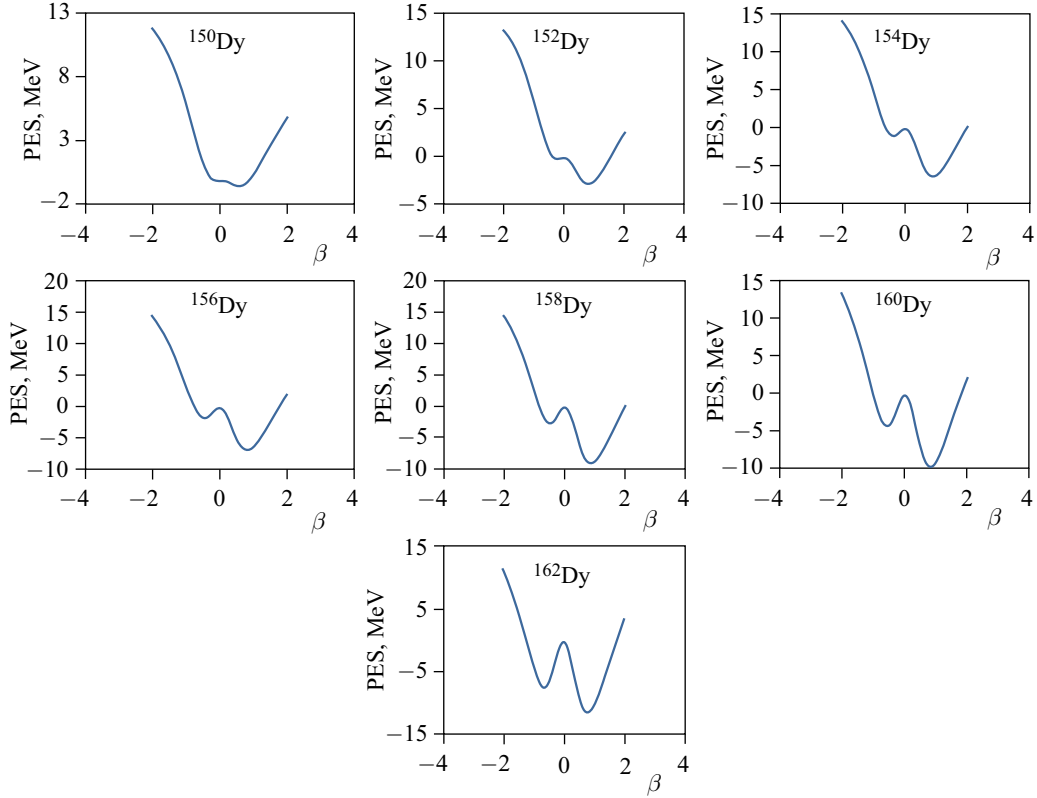


Fig. 3. Sketches of the calculated PES's as a function of deformation parameter  $\beta$  for the  $U(5)$ - $SU(3)$  transition in  $^{150-162}\text{Dy}$  isotopic chain (with  $N = 9-15$ ). The sketch at boson number  $N = 12$  represents the critical nucleus  $^{156}\text{Dy}$

Also, to identify the shape phases and their transition, it is helpful to examine the ratios of the  $E2$  reduced transition probabilities between the levels of the ground-state band. These ratios are known for  $U(5)$  and  $SU(3)$  of the IBM from the equation

$$\begin{aligned}
 B_{I+2/2} &= \frac{B(E2; I+2 \rightarrow I)}{B(E2; 2_1^+ \rightarrow 0_1^+)} = \\
 &= \begin{cases} \frac{1}{2}(I+2) \left(1 - \frac{I}{2N}\right) & \text{for } U(5), \\ \frac{15}{2} \frac{(I+2)(I+1)}{(2I+3)(2I+5)} \left(1 - \frac{I}{2N}\right) \left(1 + \frac{I}{2N+3}\right) & \text{for } SU(3). \end{cases} \quad (29)
 \end{aligned}$$

The  $E2$  operator in the IBM is given by  $T(E2) = e\hat{Q}$ , where  $\hat{Q}$  is the quadrupole operator defined in Eq. (3) and  $e$  is the effective charge. For  $^{156}\text{Dy}$  the value of  $\chi$  is  $-0.86$ , which matches the value of  $e = 0.2$ .

In Tables 2, 3 and Fig. 4, we give the comparison of the yrast excitation energy ratios  $R$  and the yrast  $B(E2)$  ratios  $B_{I+2/2}$  in the ground-state band calculated by the present model

Table 2. The energy ratios  $R_{I+2/2} = E(I+2)/E(2_1^+)$  for  $^{156}\text{Dy}$  and comparison with experimental and  $U(5)$ ,  $SU(3)$  dynamical symmetries for low-lying states

$I$	$U(5)$	$SU(3)$	$^{156}\text{Dy}$	
			Cal.	Exp.
0	1	1	1	1
2	2	3.333	3.033	2.927
4	3	7	5.809	5.579
6	4	12	9.157	8.811
8	5	18.333	12.973	12.427

Table 3. The  $B(E)$  ratios  $B_{I+2/2} = B(E2; I+2 \rightarrow I)/B(E2; 2_1^+ \rightarrow 0_1^+)$  for  $^{156}\text{Dy}$  and comparison with experimental and  $U(5)$ ,  $SU(3)$  dynamical symmetries for low-lying states

$I$	$U(5)$	$SU(3)$	$^{156}\text{Dy}$	
			Cal.	Exp.
0	1	1	1	1
2	1.833	1.4065	1.4	1.7
4	2.5	1.5054	1.8	1.5
6	3	1.5097	2.1	1.9
8	3.333	1.4619	2.3	2.5

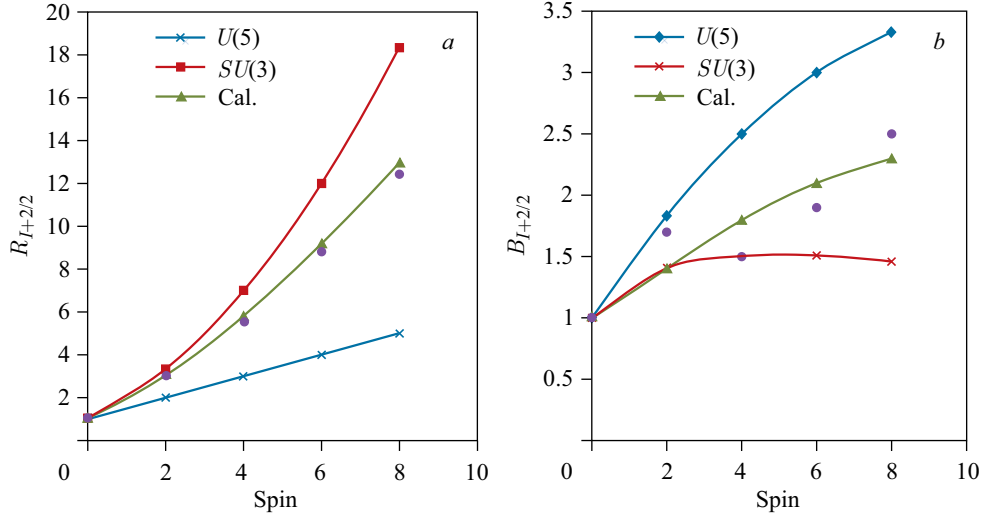


Fig. 4. Energy and  $B(E2)$  ratios for  $^{156}\text{Dy}$  and comparison with the  $U(5)$  and  $SU(3)$  limits. a) The energy ratios  $R_{I+2/2} = E(I+2)/E(2_1^+)$ . b) The  $B(E2)$  ratios  $B_{I+2/2} = B(E2; I+2 \rightarrow I)/B(E2; 2_1^+ \rightarrow 0_1^+)$ . The dots correspond to experimental values

for the critical nucleus  $^{156}\text{Dy}$  and the predictions of  $U(5)$  and  $SU(3)$  dynamical symmetry limits; furthermore, the experimental values (dots) are also represented. We can see that our calculations fit the  $X(5)$  critical point symmetry.

Besides the energy ratios and the  $E2$  transition rates, the pair transfer intensity and the two-neutron separation energies are important signatures for driven shape phase transition in even–even nuclei with respect to the total number of bosons. Calculations have been deformed for the IBM pair transfer intensities  $I_{N \rightarrow N+1}$  connecting the state in nucleus which has  $N$  bosons with the state which has  $N+1$  bosons as a function of boson number for the Dy isotopic chain ( $N_B = 9-16$ ). Tables 4a and 4b and Fig.5 illustrate the intensities between ground state–ground state ( $gs\ 0_1^+ \rightarrow gs\ 0_1^+$ ) (Fig. 4) and between ground state– $\beta$  state ( $gs\ 0_1^+ \rightarrow \beta s\ 0_2^+$ ) (Fig. 5). A comparison with the  $U(5)$  and  $SU(3)$  limits in the IBM and in boson intrinsic coherent state (BICS) is also given. A sharp rise at  $^{156}\text{Dy}$  ( $N_B = 12$ ) is seen, which is considered as a transitional nucleus in the calculations.

**Table 4a. Pair transfer intensities for Dy isotopic chain for (gs  $0_1^+ \rightarrow$  gs  $0_1^+$ )**

Symmetry limits	$N_B$						
	9	10	11	12	13	14	15
$U(5)$ (IBM)	10	11	12	13	14	15	16
$U(5)$ (BICS)	10	11	12	13	14	15	16
$SU(3)$ (IBM)	3.684	4.015	4.347	4.68	5.012	5.344	5.677
$SU(3)$ (BICS)	3.33	3.66	4	4.33	4.66	5	5.33
Cal.	10	11	12	1.666	1.623	1.513	1.475

**Table 4b. Pair transfer intensities for Dy isotopic chain for (gs  $0_1^+ \rightarrow$   $\beta s 0_2^+$ )**

Symmetry limits	$N_B$						
	9	10	11	12	13	14	15
$U(5)$ (IBM)	0	0	0	0	0	0	0
$U(5)$ (BICS)	0	0	0	0	0	0	0
$SU(3)$ (IBM)	0.6687	0.6683	0.6680	0.6678	0.6676	0.6675	0.6674
$SU(3)$ (BICS)	0.666	0.666	0.666	0.666	0.666	0.666	0.666
Cal.	0	0.75	1.4	1.15	0.9	0.7	0.68

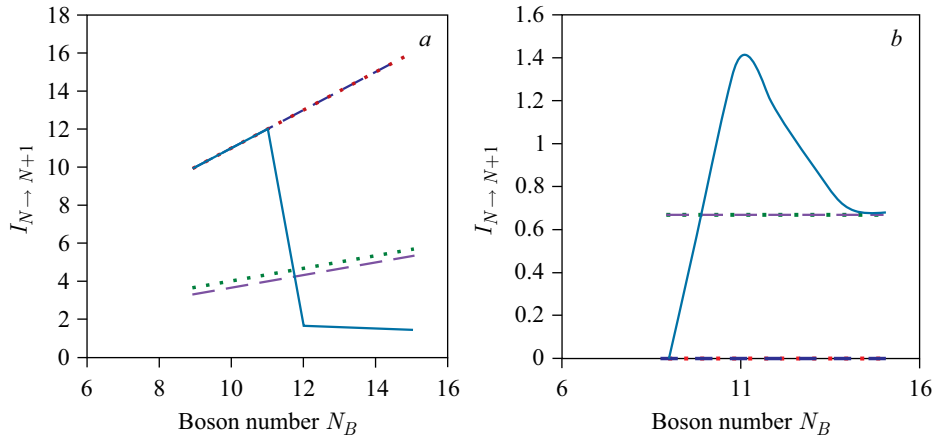


Fig. 5. Pair transfer intensities  $I_{N \rightarrow N+1}$  as a function of boson number  $N_B$  for Dy isotopic chain: a) between ground states (gs) of nuclei with  $N$  and  $N + 1$  bosons; b) between ground state of nucleus with  $N$  bosons and  $\beta$  state of nucleus with  $N + 1$  bosons

The two-neutron separation energy is defined as the energy required to remove two neutrons (one boson) from a given isotope, and for a constant proton number it is given by

$$S_{2n}(N) = BE(N) - BE(N - 1) = A + B(N - 1) + \Delta(BE), \quad (30)$$

where  $N$  is the boson number and  $A, B$  are considered to be constants along the isotopic chain and are determined by fitting procedure for Dy isotopic chain to be  $A = 17.842$  MeV and  $B = -0.156$  MeV. In Table 5 and Fig. 6, the calculations of  $S_{2n}$  match the experimentally

Table 5. The values of the two-neutron separation energies  $S_{2n}$  for Dy isotopic chain

Separation energy	$N_B$						
	9	10	11	12	13	14	15
$S_{2n}(\text{exp.})$	17.000	16.438	16.282	16.036	15.407	14.646	13.926
$S_{2n}(\text{cal.})$	16.910	16.331	16.110	15.921	15.106	14.302	13.510

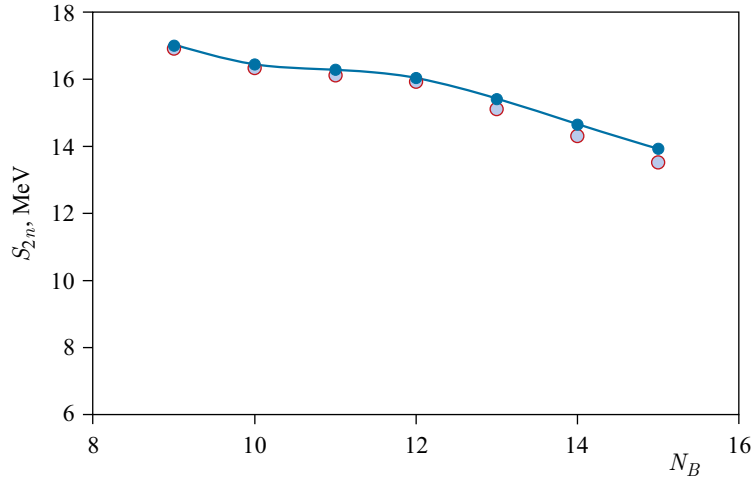


Fig. 6. Comparison between the calculated and experimental two-neutron separation energies  $S_{2n}$  for Dy isotopic chain

observed behavior. The appearance of kink in  $S_{2n}$  at  $N_B = 12$  ( $^{156}\text{Dy}$ ) indicates that the shape phase transition occurs at this point.

### CONCLUSIONS

In the present paper, we have studied the shape phase transition from a spherical vibrator  $U(5)$  to axially symmetric deformed prolate rotor  $SU(3)$  with an alternative approach in the framework of the IBM. The Hamiltonian used is composed of a single-boson energy term and a quadrupole term and contains only two parameters. We have transformed the Hamiltonian into the consistent  $\hat{Q}$  formalism (CQF) of the IBM depending on control and scaling parameters. By using the boson intrinsic coherent state, the PES's and the critical points are analyzed by varying the control parameter. The large boson number limits of the IBM at the critical points are also obtained. We have applied our results to  $^{150-162}\text{Dy}$  isotopic chain, that is known to display the first-order  $U(5)$ – $SU(3)$  shape phase transition. For each nucleus the parameters of the model have been obtained by performing the standard  $\chi^2$  fitting procedure adopted to minimize the mean square deviation between the calculated and the experimental selected low-lying excitation energies and  $B(E2)$  transition rates. The nucleus  $^{156}\text{Dy}$  has been found to be close to the critical point symmetry  $X(5)$ . The behavior of energy ratios and  $B(E2)$  ratios in the ground-state band is examined and compared to the prediction of vibrational  $U(5)$  and rotational  $SU(3)$  limits of the IBM.

## REFERENCES

1. *Iachello F., Arima A.* The Interacting Boson Model. Cambridge, England: Cambridge Univ. Press, 1987.
2. *Interacting Bose–Fermi Systems / Eds.: Casten R. F., Iachello F.* New York: Plenum, 1981.
3. *Warner D.* // *Nature*. 2002. V. 420. P. 614–620.
4. *Khalaf A. M. et al.* // *Prog. Phys.* 2015. V. 11. P. 141–145.
5. *Khalaf A. M., Taha M. M.* // *J. Theor. Appl. Phys.* 2015. V. 9. P. 127–133.
6. *Khalaf A. M., Okasha M. D.* // *Prog. Phys.* 2014. V. 10. P. 246–252.
7. *Khalaf A. M., Hamdy H. S., Elsayy M. M.* // *Prog. Phys.* 2013. V. 3. P. 44–51.
8. *Khalaf A. M., Ismail A. M.* // *Ibid.* V. 2. P. 98–104.
9. *Khalaf A. M., Awwad T. M.* // *Ibid.* V. 1. P. 7–11.
10. *Casten R. F.* // *Prog. Part. Nucl. Phys.* 2009. V. 62. P. 183–209.
11. *Barea J., Arias J. M., Garcia-Ramos J. E.* // *Phys. Rev. C*. 2010. V. 82. P. 024316.
12. *Cejnar P., Jolic J.* // *Prog. Part. Nucl. Phys.* 2009. V. 62. P. 210–256.
13. *Caprio M. A., Iachello F.* // *Nucl. Phys. A*. 2007. V. 781. P. 26–66.
14. *Niksic T. et al.* // *Phys. Rev. Lett.* 2007. V. 99. P. 092502.
15. *Alonso C. E., Arias J. M., Vitturi A.* // *Ibid.* V. 98. P. 052501.
16. *Zhang Y., Hau Z. F., Liu Y. X.* // *Phys. Rev. C*. 2007. V. 76. P. 011305(R).
17. *Leviatan A.* // *Phys. Rev. Lett.* 2007. V. 98. P. 242502.
18. *Zhao Y. et al.* // *Intern. J. Mod. Phys. E*. 2006. V. 15. P. 1711.
19. *Casten R. F.* // *Nature Phys.* 2006. V. 2. P. 811–820.
20. *Liu Y. X., Mu L. Z., Wei H. Q.* // *Phys. Lett. B*. 2006. V. 633. P. 49.
21. *Meng J. et al.* // *Eur. Phys. J. A*. 2005. V. 25. P. 23.
22. *Rowe D. J., Tunner P. S., Rosensteel G.* // *Phys. Rev. Lett.* 2004. V. 93. P. 232502.
23. *Bohr A., Mottelson B.* Nuclear Structure. V. 2. New York: Benjamin, 1975.
24. *Ginocchio J. N.* // *Nucl. Phys. A*. 1982. V. 376. P. 438.
25. *Iachello F.* // *Phys. Rev. Lett.* 2000. V. 85. P. 3580.
26. *Iachello F.* // *Phys. Rev. Lett.* 2001. V. 87. P. 052502.
27. *Iachello F.* // *Phys. Rev. Lett.* 2003. V. 91. P. 132502.
28. *Bonatsos D. et al.* // *Phys. Lett. B*. 2004. V. 588. P. 172.
29. *Dieprink A. E. L., Scholten O., Iachello F.* // *Phys. Rev. Lett.* 1980. V. 44. P. 1747.
30. National Nuclear Data Center. Data. Brookhaven Nat. Lab. Upton, NY, 2012.

Received on November 24, 2015.